

# We are IntechOpen, the world's leading publisher of Open Access books Built by scientists, for scientists

6,900

Open access books available

186,000

International authors and editors

200M

Downloads

Our authors are among the

154

Countries delivered to

TOP 1%

most cited scientists

12.2%

Contributors from top 500 universities



WEB OF SCIENCE™

Selection of our books indexed in the Book Citation Index  
in Web of Science™ Core Collection (BKCI)

Interested in publishing with us?  
Contact [book.department@intechopen.com](mailto:book.department@intechopen.com)

Numbers displayed above are based on latest data collected.  
For more information visit [www.intechopen.com](http://www.intechopen.com)



# Metamorphic Zircons Applied for Dating East African Tectono-Metamorphic Event in Central Mozambique

*Vicente Albino Manjate*

## Abstract

The term East African is now used to describe the tectonic, magmatic, and metamorphic activity of Neoproterozoic to earliest Paleozoic age. Metamorphic zircon is the most suitable geochronometer for the determination of both protolith and metamorphic ages due to its high closure temperature. The study area comprises the Mungari and Macossa-Chimoio nappes (Central Mozambique) tectonically juxtaposed to the Archaean Zimbabwe Craton. We use the metamorphic zircon morphology, Th/U ratios, and U-Pb ages to evaluate the Tectono-Metamorphic Event in central Mozambique. Morphologically, the zircon grains are sub-euhedral to euhedral, prismatic, with dark to gray cores, and narrow dark rims. The cores exhibit homogenous domains and oscillatory zoning. On the other hand, the U-Pb zircon data define Th/U ratios of 0.26–0.66 and 0.06–0.11. Finally, the U-Pb zircon analyses define upper intercept age of  $1094 \pm 36$  Ma and lower intercept age of  $498 \pm 30$  Ma. The zircon grains of the Macossa-Chimoio nappe was metamorphically re-homogenized or recrystallized by East African tectono-metamorphic event from relicts of Mesoproterozoic protolith domains. Thrusting and folding are the main East African reworking mechanisms that generated the metamorphic re-homogenization or recrystallization of the Mesoproterozoic magmatic rocks in the Macossa-Chimoio nappe of Central Mozambique.

**Keywords:** metamorphic zircon, protolith, East African, tectono-metamorphic, Macossa-Chimoio nappe, Mungari nappe

## 1. Introduction

Zircon is a fundamental secondary mineral of granitic rocks, very unsusceptible to sedimentary and metamorphic processes [1]. The term ‘metamorphic zircon’ is used to describe zircon that has formed in rocks under system-wide metamorphic conditions by a range of different processes [2]. According to [2], the main processes include precipitation from the melt during anatexis, sub-solidus nucleation and crystallization (blastogenesis) by diffusion of Zr and Si released from metamorphic breakdown reactions of major silicates and accessory phases,

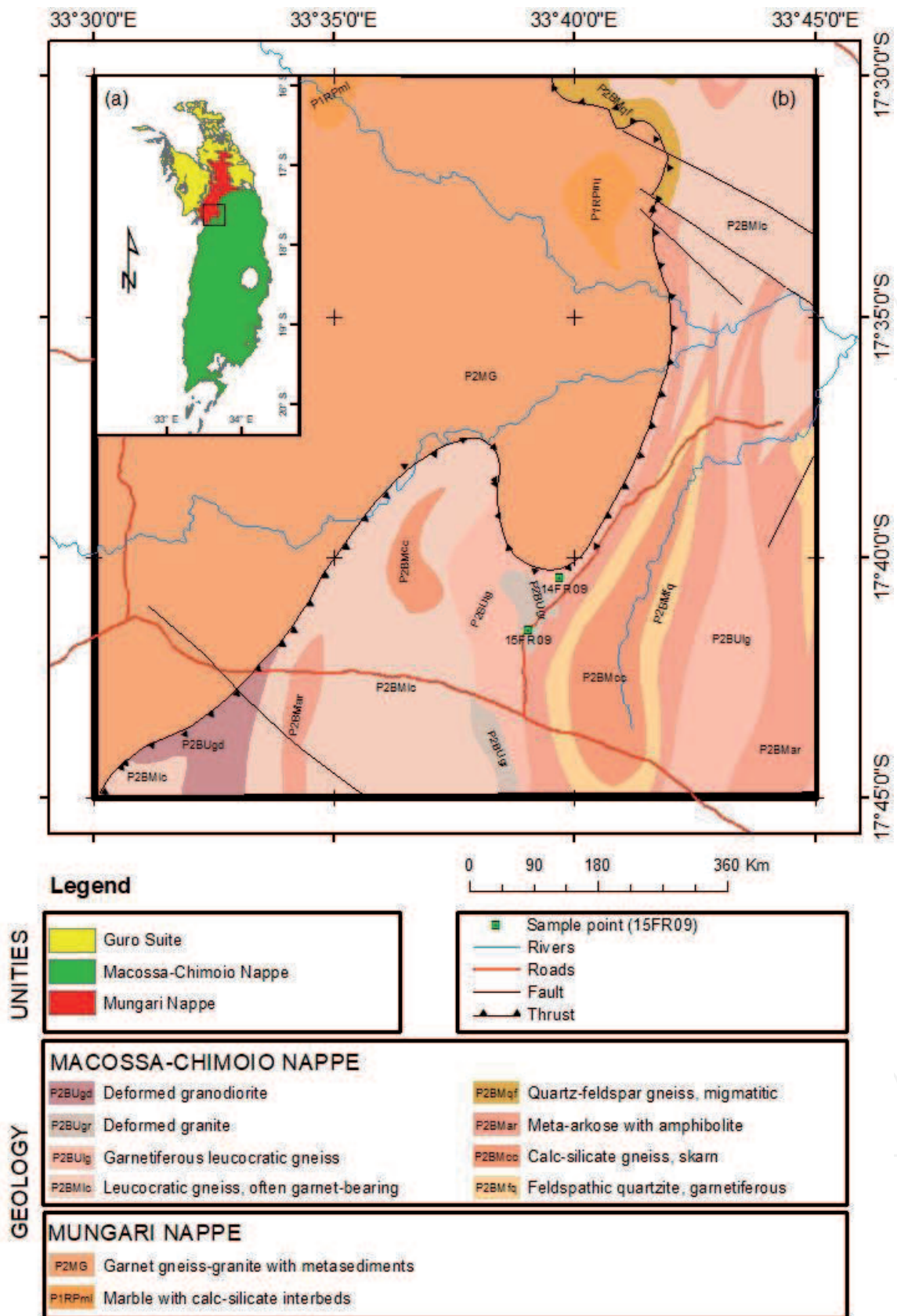


**Figure 1.** Geologic setting of the study area. (a) Regional geologic unities and (b) geology of the Macossa-Chimoio and Mungari nappes. Modified from [5–8].

precipitation from aqueous metamorphic fluid, and protolith zircon recrystallization. For these authors, knowing which process is responsible for the genesis of ‘metamorphic zircon’ in a particular sample is crucial for the correct interpretation of U-Pb isotopic data and derived ages, and consequently the interpretations of whole-rock petrogenesis.

Method	LA-ICP-MS	SHRIMP	TIMS
Applicability	• U-Pb zircon	• U-Pb zircon, titanite	• U-Pb zircon
Advantage	<ul style="list-style-type: none"> <li>• Relatively cheap;</li> <li>• Very quick (~2 min per analysis);</li> <li>• Fairly precise with an internal error of ~1%;</li> <li>• Spot size = 29 µm;</li> <li>• Excellent sensitivity, precision and good accuracy for isotope ratio measurements</li> </ul>	<ul style="list-style-type: none"> <li>• Accurate with an external error of ~1%;</li> <li>• fast with the time of analyses ~10–15 min;</li> <li>• Primary beam analytical spot size = 30 µm</li> </ul>	<ul style="list-style-type: none"> <li>• Ultrahigh precision in U-Pb dating</li> </ul>
Disadvantage	<ul style="list-style-type: none"> <li>• Does not always produce consistent results within error</li> </ul>	<ul style="list-style-type: none"> <li>• High cost partly limits its wide application</li> </ul>	<ul style="list-style-type: none"> <li>• Requires ultraclean laboratory;</li> <li>• The sample preparation is time-consuming</li> </ul>

*Modified from [11, 14, 27].*

**Table 1.**

*Summary of the applicability, advantage, and disadvantage of the LA-ICP-MS, SHRIMP, and TIMS dating techniques.*

The term East African is applied to illustrate the tectonism, magmatism, and metamorphism that took place on Neoproterozoic to earliest Paleozoic, mainly for a crust that was formally portion of Gondwana [3]. The term ‘East African’ was suggested by [4] supported on isotopic ages of Africa by Rb-Sr and K-Ar methods. According to [3], the East African was explained as a Neoproterozoic tectono-thermal event (~500 Ma) during which a number of mobile belts produced, bounding older cratons. This tectono-thermal event constitutes the final stage of an orogenic cycle, conducting to orogenic belts presently interpreted as a consequence of the fusion of continental blocks throughout the time interval from ~870 to ~550 Ma [3].

The study area comprises the nappes of Macossa-Chimoio and Mungari [5] (**Figure 1**). According to [5], the northern Mungari nappe is composed of meta-sedimentary supracrustal rocks intruded by a set of granitoid plutons. On the other hand, the southern Macossa-Chimoio nappe is composed of orthomagmatic rocks covered by medium to high-grade supracrustal rocks. In addition, both nappe complexes include detrital zircon grains with Neoproterozoic age [6].

We use the metamorphic zircon morphology, Th/U ratios, and  $^{207}\text{Pb}/^{206}\text{Pb}$  ages to evaluate the East African tectono-metamorphic event in Central Mozambique. Although the SHRIMP technique is very expensive, its advantages in comparison to other dating techniques are in favour of the geochronological data determination for this study (**Table 1**). One of the most important legacies of SHRIMP U-Pb dating on zircons is the extraction of crystallization and recrystallization ages of igneous protoliths from complexly deformed and metamorphosed lithologies.

## 2. Geological and tectonic setting

The study area (**Figure 1**) comprises rocks of the Neoproterozoic Mungari and the Mesoproterozoic Macossa-Chimoio nappes tectonically juxtaposed to the Archaean Zimbabwe Craton [5–7]. The Neoproterozoic Mungari nappe is composed of garnet gneiss-granite plutons of about 850 Ma intruding meta-sedimentary rocks consisting of marbles with calc-silicate interbeds [7]. This nappe is delimited on the west, north and east by Neoproterozoic (~850 Ma) bimodal Guro Suite and on

the south by the Macossa-Chimoio nappe [7, 8]. The Mesoproterozoic Macossa-Chimoio nappe consists of medium- to high-grade supracrustal rocks composed of quartz-feldspar gneiss, deformed granodiorite, deformed granite, garnetiferous leucocratic gneiss, meta-arkose with amphibolite, calc-silicate gneiss, feldspathic quartzite, and leucocratic gneiss [7, 8]. According to [8], in the north, the Macossa-Chimoio nappe terminates into a northward-directed arcuate thrust (**Figure 1**). For [8], the Macossa-Chimoio nappe consists of supracrustal rocks most likely derived from sedimentary precursors, originally deposited in a shallow marine paleobasin. Although the definitive character and position of all units observed within the supracrustal rocks succession are not fully solved, the overall lithostratigraphy of the paleobasin has been reduced by [8] from several geological sections made in the area [9, 10]. The lowermost rock units of the inferred paleobasin include garnetiferous leucocratic gneisses, quartz-feldspar gneisses, meta-arkoses, and arkosic quartzites. These psammitic metasediments are overlain by more pelitic rocks (metagreywackes, garnet, and sillimanite bearing mica schist and mica gneisses) with thin calc-silicate gneiss and marble interbeds.

The Macossa-Chimoio nappe is delimited by a number of structural domains. According to [8], the eastern margin of the Mesoproterozoic Macossa-Chimoio nappe is bounded by a set of rift faults/dykes 'corridor' against the Karoo and younger formations and partly remains covered by recent sediments, the western margin is a major N-S directed sinistral shear zone along the Archaean cratonic margin, in the north the nappe terminates into a northward-directed thrust, and in the south the rocks of the nappe become covered by Phanerozoic beds. According to [8], the northward thrusting of the northern part of the Macossa-Chimoio nappe over the Mungári nappe gneisses may be attributed to the East African collision, the sinistral shearing is a regional feature in the East Africa orogeny, and the set of rift faults/dykes 'corridor' against the Karoo and younger formations are normal faults with dip values commonly ranging from 45 to 60°.

The granitic pluton (deformed granite) selected for this study is located at the northern end of the Macossa-Chimoio nappe and was emplaced parallel to the foliation of the host gneisses and migmatites. The rock is a pinkish to pinkish gray, medium- to coarse-grained, weakly deformed leucogranite and is mainly composed of quartz, pinkish potassium feldspar, plagioclase, hornblende, and biotite. Accessory minerals include garnet, clinopyroxene, orthopyroxene, zircon, apatite, and opaques.

### 3. Analytical procedures

Zircon dating analyses by sensitive high-resolution ion microprobe (SHRIMP) U-Pb were performed at the São Paulo University, Brazil. This technique is very important for geochronological studies [11] as it permits *in situ* analyses of complex zircons grains often exhibiting several crystallization phases associated with different geological processes [12]. According to [12], the SHRIMP technique has an improving spatial resolution for dating with precision the different growth episodes on single zircon grains. Zircon crystals were separated utilizing the common manually breaking, crushing and grinding of samples, followed by grain size separation by sieving. The material (100–200 mesh portion) was deposited on a vibrating Wilfley table, and heavy minerals were then densimetrically separated using bromoform ( $d = 2.89 \text{ g/ml}$ ; 20°C) and methylene iodide ( $d = 3.32 \text{ g/ml}$ ; 20°C). The dense material (density above 3.32 g/ml) was then electromagnetically separated using a Frantz separator. The magnetic minerals were separated using a hand magnet and the paramagnetic minerals were separated by a Frantz

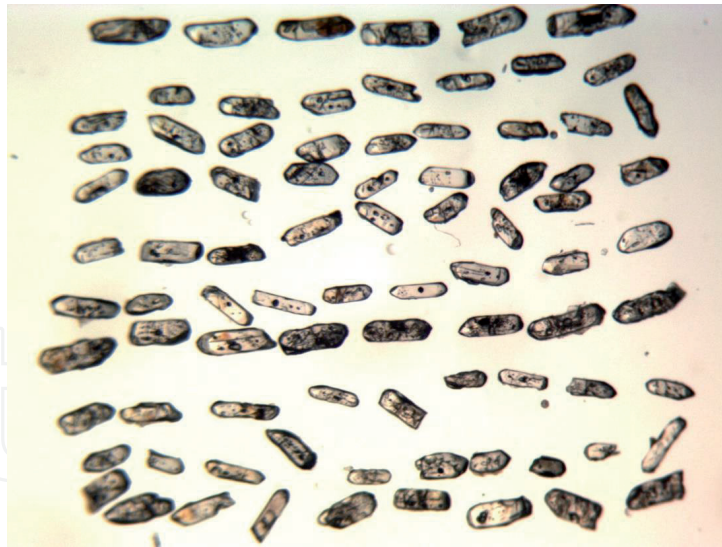


**Figure 2.**  
Reflected and transmitted light images of the deformed granite zircons. Photograph length of 2.3 mm.

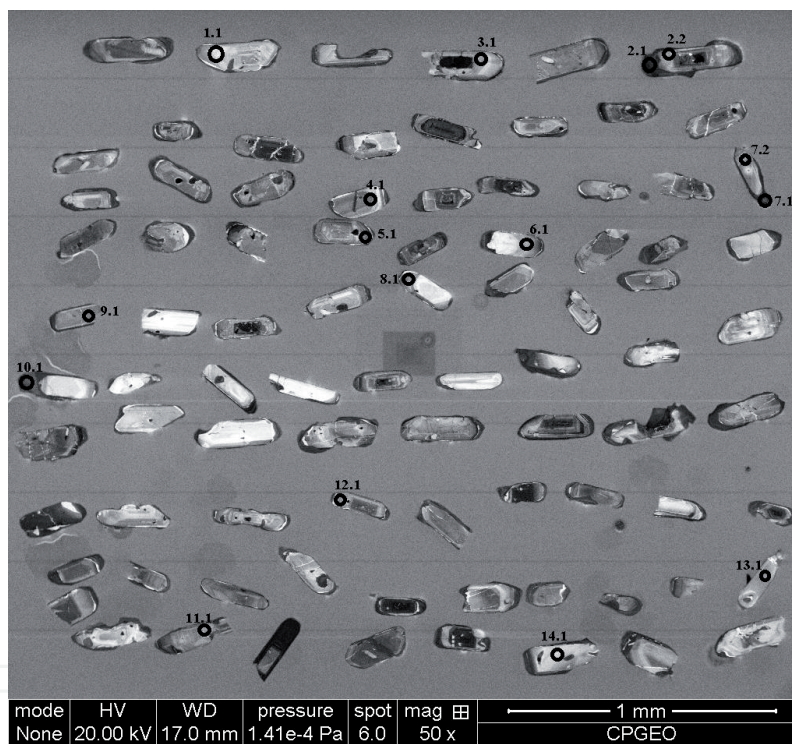


**Figure 3.**  
CL image of zircons with selected analyses locations (spots) by SHRIMP IIe/MC.

magnetic separator (amperage variation). Zircon crystals are concentrated in the non-magnetic portion. Zircon crystals along with zircon standards were picked by hand, impregnated in epoxy resin mounts with a diameter of 2.54 cm, ground and polished with diamond compound (1–7  $\mu\text{m}$ ) to reveal grain centers and carbon coated as well as cleaned and gold-coated in preparation for the SHRIMP analyses. Reflected and transmitted light images (**Figure 2**) were acquired before the gold coating of 2–3  $\mu\text{m}$ . Zircons internal structures were microphotographed in transmitted and reflected light and characterized by the use of cathodoluminescence (CL) images from scanning electron microscope prior to SHRIMP U-Pb zircon isotopic analyses. CL images of representative zircon crystals can be seen in **Figure 3**. After CL acquisition, the gold was removed and the mount was re-cleaned. The U-Pb zircon dating analyses were made using a SHRIMP IIe/MC mass spectrometer

Spot	<sup>206</sup> Pbc (%)	U (ppm)	Th (ppm)	<sup>232</sup> Th/ <sup>238</sup> U	<sup>206</sup> Pb* (ppm)	Ages (Ma) corrected to <sup>204</sup> Pb				Disc (%)	Ratios corrected to <sup>204</sup> Pb				Error correl
						<sup>206</sup> P/ <sup>238</sup> U	Error (%)	<sup>207</sup> Pb/ <sup>206</sup> Pb	Error (%)		<sup>207</sup> Pb*/ <sup>235</sup> U	Error (%)	<sup>206</sup> Pb*/ <sup>238</sup> U	Error (%)	
Amostra 15FR09															
1.1c	0.19	127	55	0.44	21.6	1159.5	15.0	1102	77	-5	2.07	4.1	.1971	1.4	.346
2.1r	0.01	890	88	0.10	61.3	497.0	5.8	542	16	9	0.64	1.4	.0801	1.2	.861
2.2c	0.38	275	69	0.26	31.3	799.9	15.9	875	43	9	1.24	3.0	.1321	2.1	.714
3.1c	0.06	175	74	0.43	27.7	1090.8	13.0	1136	19	4	1.97	1.6	.1844	1.3	.804
4.1c	-0.05	210	100	0.49	30.5	1006.4	12.0	1053	30	5	1.73	2.0	.1690	1.3	.656
5.1c	0.14	472	133	0.29	65.5	963.1	11.0	971	23	1	1.59	1.7	.1611	1.2	.740
6.1c	0.05	206	94	0.47	27.6	933.4	11.8	1030	27	10	1.58	1.9	.1558	1.4	.708
7.1r	0.39	942	56	0.06	69.0	525.8	6.2	515	38	-2	0.67	2.1	.0850	1.2	.580
7.2c	0.07	243	135	0.57	39.9	1127.8	13.1	1114	15	-1	2.02	1.5	.1912	1.3	.856
8.1c	0.06	279	98	0.36	42.6	1056.0	13.9	1136	16	8	1.90	1.6	.1780	1.4	.871
9.1c	0.05	275	165	0.62	39.7	1000.6	11.6	1057	14	6	1.73	1.4	.1679	1.2	.871
10.1r	0.20	860	95	0.11	59.4	497.7	5.8	510	23	2	0.64	1.6	.0803	1.2	.755
11.1c	0.29	238	97	0.42	26.5	782.2	9.5	872	31	11	1.21	2.0	.1290	1.3	.650
12.1c	0.09	288	111	0.40	44.2	1060.1	12.5	1115	16	5	1.89	1.5	.1787	1.3	.847
13.1c	0.15	250	145	0.60	34.4	957.5	11.3	1025	23	7	1.62	1.7	.1601	1.3	.751
14.1c	0.32	110	70	0.66	17.1	1066.0	13.2	1032	35	-3	1.83	2.2	.1798	1.3	.610

\*Total radiogenic.

**Table 2.**  
Analytical data for zircons from the deformed granite, Macossa-Chimoio nappe.

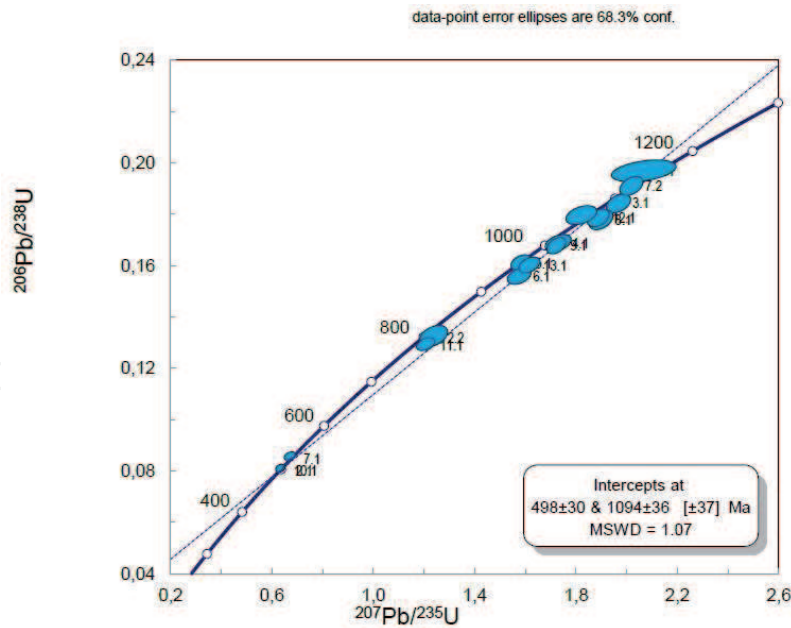


**Figure 4.** Concordia diagram of zircon U-Pb isotope data analyzed by SHRIMP IIe/MC for the deformed granite, Macossa-Chimoio nappe.

and zircon standards designated Temora 2 [13]. As described in [14], this consisted of measuring U, Pb and Th abundances, and isotopic relationships of these elements in zircon crystals. The precision of the U, Pb and Th zircons analytical data obtained by SHRIMP IIe at São Paulo University Laboratory is of the same standard when compared to the data from leading laboratories worldwide [14]. The reduction of raw data was carried out using SQUID 1.06 [15]. Common lead corrections usually use  $^{204}\text{Pb}$  according to [16].

The U-Pb zircon dating results are shown in **Table 2** and projected in the Concordia diagram (see **Figure 4**). There is evidence of recrystallized domains and inherited cores on CL images. Results from recrystallized domains and inherited cores were not used in the final age determination. Results above 10% discordance ( $1\sigma$ ) and/or with extremely big errors originated by a correction of common lead were also not used in the final age determination. Age determination and Concordia diagram processed using ISOPLOT of version 4.0 [15]. Errors shown in **Table 2** and **Figure 4** are  $1\sigma$  levels. In a situation of evident Pb-loss, consecutive younger results were discarded until obtaining an acceptable mean square of weighted deviations (MSWD). The remaining U-Pb zircon dating results were used to determine the magmatic and metamorphic ages. All age errors in the text and Concordia diagram are considered at ( $1\sigma$ ).

## 4. Results and discussions

### 4.1 Zircon morphology and internal structure

Zircon morphology and internal structure provide an important tool for discerning their growth stages and genesis. Zircons of our study are products of anatectic melt, altered by metamorphic fluid and hydrothermal alteration. Anatectic melt, metamorphic fluid, and hydrothermal alteration are important factors controlling the morphology and internal structure of zircons overgrowths [17]. Zircons crystallizing from anatectic melts also have a euhedral shape with no zoning, planar zoning or oscillatory zoning. In addition, zircons altered by the metamorphic fluid

are usually homogenous with high CL intensity, showing resorption structure. Moreover, zircon domains that lost all radioactive Pb during hydrothermal alteration always show white color in CL image. The study made on deformed granite showed that the zircon grains are inherited from older crustal rocks or metamorphically re-homogenized or recrystallized from relicts of magmatic protolith domains. These zircon grains range in size from 250 to 400  $\mu\text{m}$  of length, and 125  $\mu\text{m}$  of width with length/width ratios of 2:1–3.2:1. In addition, they are colorless and transparent (**Figure 2**), sub-euhedral to euhedral with elongated prismatic shapes. Moreover, these zircon grains exhibit narrow dark rims and dark to gray cores with some homogenous domains and other domains of compositional or oscillatory zoning (**Figure 3**), being thus strongly re-homogenized. Therefore, the zircons of our study are products of anatectic melts or altered by metamorphic and hydrothermal fluids.

#### 4.2 Genesis and recrystallization of the metamorphic zircons

Sixteen analyses spots (cores and rims) in 14 zircon grains from the deformed granite for Th/U ratios and  $^{207}\text{Pb}/^{206}\text{Pb}$  ages determinations (**Table 2**). These analyses spots define two groups based on Th/U ratios and apparent  $^{207}\text{Pb}/^{206}\text{Pb}$  ages. The first group is defined by cores with U grades from 110 to 472 ppm (averaging 242 ppm) and Th ranging from 55 to 165 ppm (averaging 104 ppm). This result in Th/U ratios from 0.26 to 0.66 and  $^{207}\text{Pb}/^{206}\text{Pb}$  ages varying from  $872 \pm 31$  to  $1136 \pm 19$  Ma. The other group is represented by rims with U grades ranging from 860 to 942 ppm (average of 890 ppm) and Th ranging from 56 to 95 ppm (average of 80 ppm). This result in Th/U ratios from 0.06 to 0.11 (average of 0.09) and  $^{207}\text{Pb}/^{206}\text{Pb}$  ages varying from  $510 \pm 23$  to  $542 \pm 16$  Ma. The age data follow a regression line (**Figure 4**) that allowed to determine the upper intercept age of  $1094 \pm 36$  Ma and lower intercept age of  $498 \pm 30$  Ma (MSWD = 1.07).

Th/U ratios are used as indicators of zircon types. The Th/U ratios of magmatic zircons are commonly between 0.32 and 0.70, whereas hydrothermal zircons frequently have more extreme values [18–20]. Proposed that Th/U ratios  $<0.1$  are probably a hint for hydrothermal origin. Therefore, the studied zircons are products of metamorphic re-homogenization or recrystallization from relicts of magmatic protoliths.

The studied metamorphic zircons registered two events. The magmatic protolith domains crystallized at  $\sim 1094 \pm 36$  Ma. This was followed by re-homogenization or recrystallization related to northward-directed thrusting and folding at  $\sim 498 \pm 30$  Ma of the Chimoio-Macossa nappe [5]. Using LA-ICP-MS U/Pb zircon for leucocratic gneiss (sample 14FR09, **Figure 1**) of Chimoio-Macossa nappe found  $^{207}\text{Pb}/^{206}\text{Pb}$  crystallization age of  $1067.8 \pm 9.0$  Ma and a metamorphic age of  $504 \pm 1.8$  Ma. These age determinations are in accordance with that of [21] for the Macossa-Chimoio nappe. According to Yuanbao (2004), the time of metamorphic recrystallization is represented by the age of recrystallized zircon domain with the lowest Th/U ratio and the youngest U-Pb age.

The Cambrian U-Pb ages are found in both cores and rims of the Mesoproterozoic Macossa-Chimoio nappe rocks. Manjate [22] found a Neoproterozoic-Cambrian recrystallization age ( $498 \pm 19$ – $562 \pm 14$  Ma) on zircon cores of the Dongueni Mount nepheline syenite generated from partial melting of Mesoproterozoic crust, as shown by inherited zircon ages of  $1040 \pm 14$  (15) Ma. The Cambrian magmatism, defined by zircon U-Pb dates of c. 490 Ma, from Dongueni Mount nepheline syenite, southeast of Chimoio village [23], is post-collisional and marks the end stage of East African Orogeny. Therefore, zircons are suitable for dating the tectono-metamorphic Neoproterozoic-Cambrian event that affected the Macossa-Chimoio nappe. The Neoproterozoic-Cambrian recrystallization ages on zircon were the common determinations made by a number of authors [23–26].

## 5. Conclusions

Zircons are appropriate for dating the tectono-metamorphic Neoproterozoic-Cambrian event that affected the Macossa-Chimoio nappe. The studied zircon grains exhibit narrow dark rims and dark to gray cores with some homogenous domains and other domains of compositional or oscillatory zoning, as well as, Th/U ratios less than 0.3 which are evidence of metamorphic re-homogenization or recrystallization from relicts of magmatic protolith domains.

Thrusting and folding are the main East African Neoproterozoic-Cambrian reworking mechanisms (ca.  $498 \pm 30$  Ma) that generated the metamorphic re-homogenization or recrystallization of the Mesoproterozoic magmatic rocks (ca.  $1094 \pm 36$  Ma) in the Macossa-Chimoio nappe of Central Mozambique.

## Acknowledgements

This study results from the PhD project involving the cooperation of institutions (CNPQ and PRO-AFRICA, Brazil, and the National Institute of Mines, Mozambique) in the form of financial support and services. The author thanks Centro de Pesquisas Geocronológicas (CPGeo) of IGc/USP for the U-Pb zircon analyses and anonymous reviewers for their careful comments that have improved the manuscript remarkably.

## Conflict of interest

The author declares that there is no conflict of interest.

## Author details

Vicente Albino Manjate  
National Institute of Mines, Maputo, Mozambique

\*Address all correspondence to: [vmanjate@yahoo.com.br](mailto:vmanjate@yahoo.com.br)

## IntechOpen

© 2019 The Author(s). Licensee IntechOpen. This chapter is distributed under the terms of the Creative Commons Attribution License (<http://creativecommons.org/licenses/by/3.0>), which permits unrestricted use, distribution, and reproduction in any medium, provided the original work is properly cited. 

## References

- [1] Martins HCB, Simões PP, Abreu J. Zircon crystal morphology and internal structures as a tool for constraining magma sources: Examples from northern Portugal Variscan biotite-rich granite plutons. *Comptes Rendus Geoscience*. 2014;**346**:233-243
- [2] Hoskin PWO, Black LP. Metamorphic zircon formation by solid-state recrystallization of protolith igneous zircon. *Journal of Metamorphic Geology*. 2000;**18**:423-439
- [3] Kröner A, Stern RJ. Pan-African Orogeny. Africa. *Encyclopedia of Geology*. Vol. 1. Amsterdam: Elsevier; 2004. pp. 1-12
- [4] Stern RJ. ARC assembly and continental collision in the neoproterozoic east african orogen: Implications for the consolidation of gondwanaland. *Annual Review of Earth and Planetary Sciences*. 1994;**22**:319-351. DOI: 10.1146/annurev.ea.22.050194.001535
- [5] Chaúque FR, Cordani UG, Jamal DL. Geochronological systematics for the Chimoio-macossa frontal nappe in Central Mozambique-implications for the tectonic evolution of the southern part of the Mozambique belt. *Journal of the African Earth Sciences*. 2019;**150**:47-67. DOI: 10.1016/j.jafrearsci.2018.10.013
- [6] Chaúque FR, Cordani UG, Jamal DL, Onoe AT. The Zimbabwe craton in Mozambique: A brief review of its geochronological pattern and its relation to the Mozambique belt. *Journal of the African Earth Sciences*. 2017;**129**:366-379. DOI: 10.1016/J.JAFREARSCI.2017.01.021
- [7] Chaúque FR. Contribuição para o conhecimento da evolução tectônica do Cinturão de Moçambique, em Moçambique. *Biblioteca Digital de Teses e Dissertações da Universidade de São Paulo*; 2012. DOI: 10.11606/T.44.2012.tde-02062015-152355
- [8] GTK Volume II. Map explanation: Sheets 1630-1934. *Geology of Degree Sheets Mecumbura, Chioco, Tete, Tambara, Guro, Chemba, Manica, Catandica, Gorongosa, Rotanda, Chimoio and Beira*; Maputo:vol. 2; 2006
- [9] Hunting. Ground geophysics. mineral inventory project in tete province and parts of manica, sofala and zambezia provinces. Report on ground geophysics investigations for the period July to October 1982; Maputo: 1983
- [10] Hunting. Mineral inventory project in tete province and parts of manica, sofala and zambezia provinces. Report on ground geophysical investigations for the 1982 and 1983 field season; Maputo: 1984
- [11] Sato K, Junior OS, MAS B, CCG T, Onoe AT. SHRIMP U-Th-Pb analyses of titanites: Analytical techniques and examples of terranes of the south-southeast of Brazil: *Geoscience Institute of the University of São Paulo. Geologia USP. Série Científica*. 2016;**16**:3-18. DOI: 10.11606/issn.2316-9095.v16i2p3-18
- [12] Chemale F Jr, Kawashita K, Dussin IA, Ávila JN, Justino D, Bertotti A. U-Pb zircon in situ dating with LA-MC-ICP-MS using a mixed detector configuration. *Annals of the Brazilian Academy of Sciences*. 2012;**84**:275-295
- [13] Black LP, Kamo SL, Allen CM, Davis DW, Aleinikoff JN, Valley JW, et al. Improved  $^{206}\text{Pb}/^{238}\text{U}$  microprobe geochronology by the monitoring of a trace-element-related matrix effect; SHRIMP, ID-TIMS, ELA-ICP-MS and oxygen isotope documentation for a series of zircon standards. *Chemical Geology*. 2004;**205**:115-140. DOI: 10.1016/j.chemgeo.2004.01.003
- [14] Sato K, Tassinari CCG, Basei MAS, Siga Júnior O, Onoe AT, de

- Souza MD. Sensitive high resolution ion microprobe (SHRIMP IIe/MC) of the institute of geosciences of the University of São Paulo, Brazil: Analytical method and first results. *Geologia USP. Série Científica*. 2014;**14**:3-18. DOI: 10.5327/Z1519-874X201400030001
- [15] Ludwig KR. User's Manual for Isoplot 3.00: A Geochronological Toolkit for Microsoft Excel. Berkeley CA: Special publication/Berkeley Geochronology Center; 2003
- [16] Stacey JS, Kramers JD. Approximation of terrestrial lead isotope evolution by a two-stage model. *Earth and Planetary Science Letters*. 1975;**26**:207-221. DOI: 10.1016/0012-821X(75)90088-6
- [17] Yuambao W, Yongfei Z. Genesis of zircon and its constraints on the interpretation of U-Pb age. *Chinese Science Bulletin*. 2004;**49**:1554. DOI: 10.1360/04wd0130
- [18] Fu B, Mernagh TP, Kita NT, Kemp AIS, Valley JW. Distinguishing magmatic zircon from hydrothermal zircon: A case study from the Gidginbung high-sulphidation Au-Ag-(Cu) deposit, SE Australia. *Chemical Geology*. 2009;**259**:131-142. DOI: 10.1016/J.CHEMGEO.2008.10.035
- [19] Rubatto D. Zircon trace element geochemistry: Partitioning with garnet and the link between U-Pb ages and metamorphism. *Chemical Geology*. 2002;**184**:123-138. DOI: 10.1016/S0009-2541(01)00355-2
- [20] Hoskin PWO, Schaltegger U. The composition of zircon and igneous and metamorphic petrogenesis. *Reviews in Mineralogy and Geochemistry*. 2003;**53**:27-62. DOI: 10.2113/0530027.
- [21] Fritz H, Abdelsalam M, Ali KA, Bingen B, Collins AS, Fowler AR, et al. Orogen styles in the east African orogen: A review of the Neoproterozoic to Cambrian tectonic evolution. *Journal of the African Earth Sciences*. 2013;**86**:65-106. DOI: 10.1016/j.jafrearsci.2013.06.004
- [22] Manjate VA. Whole-rock geochemical, U-Pb and Sm-Nd isotope characteristics of the Dongueni Mont nepheline syenite intrusion, Mozambique. *Geoscience Frontiers*. 2015;**8**:1063-1071. DOI: 10.1016/j.gsf.2016.10.009
- [23] Manjate VA. Geocronologia da região de Gondola-Nhamatanda (Centro de Moçambique). *Biblioteca Digital de Teses e Dissertações da Universidade de São Paulo*; 2012. DOI: 10.11606/D.44.2012.tde-21122012-085416
- [24] Manjate VA. Caracterização geocronológica dos granitóides do complexo de bárué e da suíte de guro, centro-oeste de moçambique: Implicações tectônicas e metalogenéticas. *Biblioteca Digital de Teses e Dissertações da Universidade de São Paulo*; 2015. DOI: 10.11606/T.44.2015.tde-22122015-143300
- [25] Manjate VA. U-Pb zircon geochronology and Sr-Nd isotopic composition of the Inchope orthogneiss in Mozambique: Age constraints and petrogenetic implications. *Journal of the African Earth Sciences*. 2017;**131**:98-104. DOI: 10.1016/j.jafrearsci.2017.03.027
- [26] Manjate VA, Tassinari CCG. Zircon U-Pb geochronology and Nd isotope systematics of the Guro suite granitoids, Mozambique: Implications for Neoproterozoic crust reworking events. *Journal of the African Earth Sciences*. 2018;**148**:69-79. DOI: 10.1016/j.jafrearsci.2018.05.012
- [27] Becker JS. State-of-the-art and progress in precise and accurate isotope ratio measurements by ICP-MS and LA-ICP-MS: Plenary lecture. *Journal of Analytical Atomic Spectrometry*. 2002;**17**:1172-1185. DOI: 10.1039/B203028B